PHYSICAL REVIEW A **80**, 010501(R) (2009)

Measurement of the *D*-line doublet in high-*Z* highly charged sodiumlike ions

J. D. Gillaspy,[1] I. N. Draganić,[1] Yu. Ralchenko,[1] J. Reader,[1] J. N. Tan,[1] J. M. Pomeroy,[1] and S. M. Brewer[1,2]
[1]*Atomic Physics Division, National Institute of Standards and Technology, Gaithersburg, Maryland 20899-8422, USA*
[2]*Chemical Physics Program, University of Maryland, College Park, Maryland 20742, USA*
(Received 20 March 2009; published 8 July 2009)

We report a direct observation of the *D*-line doublet of Na-like ions with $Z \geq 72$. Spectra in the 1–9 nm spectral range are presented showing the widely split doublet for Hf^{61+}, Ta^{62+}, W^{63+}, and Au^{68+}. The ions were produced and confined in an electron-beam ion trap and observed with a flat-field grazing incidence spectrometer. The measured wavelengths agree well with the predictions of relativistic many-body perturbation theory with QED corrections. We also report the measured wavelengths for several transitions in Si-, Al-, and Mg-like ions of Hf, Ta, and W and in Mg-like Au.

DOI: 10.1103/PhysRevA.80.010501 PACS number(s): 32.30.Rj, 31.30.jc, 32.10.Fn, 32.70.Fw

The *D* lines in sodium (D_1 and D_2 correspond to transitions of the valence electron to the $3s_{1/2}$ ground state from the first excited states, $3p_{1/2}$ and $3p_{3/2}$, respectively), are among the most well-known atomic emission lines in science and industry. They are widely used in applications that range from the mundane, such as street lighting [1], to the exotic, such as Bose-Einstein condensates and atom lasers [2]. Part of the attraction to the *D* lines is that their intensities are approximately one hundred times larger than those of any other sodium line in the visible region of the electromagnetic spectrum [3]. Hence, for many applications, nearly all of the light from sodium comes from these two strong lines. The highly charged counterparts to sodium, the Na-like ions, figure prominently in the diagnostics of fusion energy devices [4,5] and in astronomy [6], where temperatures in excess of 10^7 K are encountered.

The splitting of the *D* line doublet rapidly increases along the isoelectronic sequence due to a strong dependence on the nuclear charge *Z* (more precisely the ion core charge $Z_c = Z - 10$). In the nonrelativistic limit, the $3p_{1/2}$ and $3p_{3/2}$ levels are degenerate [7], and it is relativistic effects such as the spin-orbit interaction accompanied at higher *Z* by the effects of quantum electrodynamics (QED) that are responsible for the observed splitting. In neutral Na, the splitting is only one part in a thousand but with increasing nuclear charge the splitting grows more rapidly than the energies. For $Z > 70$, the splitting becomes greater than the mean energy of the doublet, making it difficult to measure both lines simultaneously with a single spectrometer.

Before the present work, the highest Na-like ion for which wavelengths of both *D* lines were available was $Z=54$ [8–10]. Moreover, there are only a few experiments that yielded measurements of either the D_1 or the D_2 lines for elements beyond $Z=54$. Measurements of the D_2 line have been published at $Z=55$ [11], $Z=64$ [12], $Z=78$ [13], $Z=82$ [14,15], and $Z=92$ [16], and the D_1 line was measured at $Z=79$ [17]. The difficulty of measuring these lines at high *Z* is evidenced by the remarks of Simionovici *et al.* [14] who note in their paper that a major effort was required in their beam-foil experiment to get a signal-to-noise ratio of approximately unity. Recently, we reported a relatively high signal-to-noise measurement of the D_1 lines in the range $Z=72$ to $Z=79$ [18], but the D_2 line fell outside the wavelength range of the spectrometer. Thus, a direct observation of the splitting of the *D* lines in sodiumlike ions is nonexistent for the upper part of the periodic table. To remedy this situation, we modified the grazing incidence spectrometer used in our previous work [18], extending its range from the extreme ultraviolet down into the soft x-ray range, and used it to observe simultaneously the D_1 and D_2 lines at $Z=72$, 73, 74, and 79.

In a series of measurements, one for each of the four elements studied, low charge metal ions from a multicathode metal vapor vacuum arc (MEVVA) [19] were injected into the electron-beam ion trap (EBIT) [20] at NIST and ionized to high charge states by impact with a 150 mA electron beam accelerated through an applied potential of 12 kV (24 kV for Au). The 2.7 T magnetic induction inside the trap compressed 80% of the beam current to a diameter of 60 μm [21], yielding an average electron density inside this diameter of 9×10^{12} cm^{-3}. The average electron density experienced by the ions may be five times lower [22] due to the fact that the hot (of order 10^7 K) ion cloud has a diameter considerably larger [23] than that of the electron beam.

The extreme ultraviolet (euv) spectrometer used in the present work was modified from an earlier configuration [24] by translating the charge coupled device (CCD) in the focal plane in order to capture photons that are diffracted at small angles. This pushed the instrument beyond its optimal flat-field design specifications but allowed the observation of wavelengths as short as 1.6 nm (770 eV), closing the gap that previously existed between the coverage of this spectrometer and the microcalorimeter used in our earlier x-ray work [25]. In recalibrating the spectrometer, 11 previously used [24] long-wavelength reference lines from Li-like and Be-like Ne, and Ne-like Ar were supplemented with lines from H-like and He-like carbon, nitrogen, and oxygen [3]. Several of these lines were also used in higher orders.

Photons were collected continuously in 1200 s blocks, during which 1340 column-summed CCD wavelength channels were read and stored every 60 s in order to facilitate the removal of cosmic ray events. Every 10 s, the trap potential was lowered to 9.8 kV for 10 ms to empty and reload a new batch of ions. An axial trap potential of 220 V was applied. No evaporative cooling gas was injected for Hf, Ta, and W, and the residual background pressure was about 10^{-8} Pa or lower. Under these conditions, the time required for sequential ionization to the Na-like charge state is estimated to be approximately an order of magnitude smaller than the 10 s trap reload period. For the Au measurements, molecular nitrogen was used for cooling. The number of 1200 s blocks of

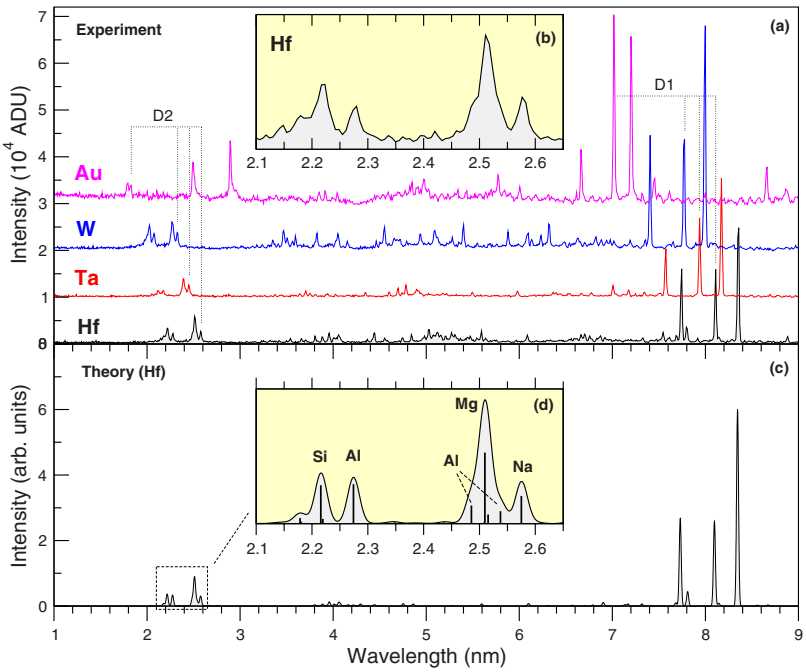

FIG. 1. (Color online) (a) Measured spectra of Hf, Ta, and W at the nominal beam energy of 12 keV and Au at 24 keV. (b) Measured spectrum of Hf between 2.1 and 2.65 nm. (c) Calculated spectrum of Hf. (d) Calculated spectrum of Hf between 2.1 and 2.65 nm showing positions and ion stages for the strongest lines. ADU stands for analog-to-digital units of the CCD detector.

data summed to produce the spectra discussed below was 6.5 (Hf), 6 (Ta), 13 (W), and 19 (Au).

In our previous publications [18,26,27] we emphasized the significance of accurate collisional-radiative modeling to interpret the spectra. This approach allowed us to identify numerous spectral lines from highly charged ions of heavy elements. In the present work, we make use of the collisional-radiative code NOMAD [28] with a realistic non-Maxwellian electron energy distribution appropriate to the EBIT [18]. The input atomic data (energy levels, transition probabilities, and collisional cross sections) for NOMAD was calculated using the FAC code [29]. Nearly 4000 energy levels in 8 ionization stages and 1.25×10^6 collisional and radiative transitions were calculated for each of the elements studied. In addition to electron-impact and radiative processes, the simulations also include charge exchange (CX) recombination of the highly charged ions with the neutrals present in the EBIT. Since the density and relative velocity of the gas molecules and ions are not precisely known, their product was used as the only adjustable parameter in the simulations. As in Ref. [18], we used classical trajectory Monte Carlo values for the CX cross sections. Due to the possibility of an incompletely neutralized space-charge correction [23], the actual electron-beam energy may be somewhat different than the nominal beam energy that we assume in the calculation, but the small differences from the assumed beam energy are compensated by adjustments of the density-velocity parameter.

The measured spectra of Hf, Ta, Au, and W are shown in Fig. 1(a). The CCD bias offset of approximately 7000 counts/channel per block has been subtracted. For better visibility, the Ta, W, and Au spectra are shifted upwards by 10 000, 20 000, and 30 000 counts, respectively. Two separated groups of strong lines are clearly identified in the figure. The spectral lines near 8 nm, including the D_1 line in Na-like ions, were studied in our recent publication [18]. The other set of strong lines at short wavelengths (below 2.6 nm) originate from Si-to Na-like ions, with the D_2 line having the longest wavelength. The prominent spectral features at 2.5 and 2.9 nm in the Au spectrum come from nitrogen ions.

Shown in Fig. 1(c) is an example of a calculated Hf spectrum adjusted for the spectrometer instrument function. The instrument function is based on the grating efficiency [30], the calculated mirror reflectivity [31], the CCD detector quantum efficiency [32], the observed spectrometer resolution [0.02 nm full width at half maximum (FWHM) linewidth], and the conversion of photon number to line intensity (energy detected per unit bandwidth) [7]. In these measurements there was no window between the spectrometer and the trapped ions. The observed line ratios of the three strongest lines near 8 nm were reproduced by adjusting the CX density-velocity product to 9×10^{14} s^{-1} cm^{-2} for an assumed electron density of 1×10^{12} cm^{-3}. The ratio of the D_2 to D_1 integrated line intensity for the case of Hf is 0.16(8) (experiment) and 0.10 (theory). Without the applied instrument function, the calculated number of photons emitted into the D_2 line in Hf, relative to the D_1 line, is 1.5. Other than our results here and in Ref. [9], the relative intensity information on the D doublet at high-Z appears to be rather scarce in the spectroscopy literature. In the papers reviewed by Reader *et al.* [33], for example, the heaviest element for which relative intensity information is available is iron ($Z=26$).

To the best of our knowledge, there are two sets of extensive calculations for the D lines covering a large range of nuclear charges. Kim *et al.* [34] used multiconfiguration Dirac-Fock (MCDF) and relativistic many-body perturbation theory (RMBPT) to obtain relativistic correlation energies that were then used together with phenomenological estimates of the QED effects to derive the transition energies for $Z=14$ to $Z=92$. Reference [34] also contains a thorough discussion of available experimental data and their trends. Blundell [35] combined RMBPT [36] results with a more comprehensive *ab initio* calculation of the leading QED terms and reported D-line wavelengths for nine elements from Z

TABLE I. Measured wavelengths (in nm) of D_1 and D_2 lines and corresponding theoretical and semiempirical predictions. The numbers shown in the first and second sets of parentheses after the wavelengths are the estimated uncertainties (at the "one-σ" or 68% confidence level here and throughout this work) associated with statistical and systematic errors, respectively. The numbers shown in parenthesis for the column labeled "D_{1av}" are the total uncertainties for the weighted average of our present and previous results [18].

Ion	This experiment	Ref. [18]	D_{1av}	MCDF [34]	FAC	Semiemp. [12]
D_2 $3s_{1/2}$-$3p_{3/2}$						
Hf^{61+}	2.5769(7)(15)			2.5771	2.5747	2.5760
Ta^{62+}	2.4496(10)(15)			2.4479	2.4457	2.4469
W^{63+}	2.3243(7)(15)			2.3255	2.3235	2.3245
Au^{68+}	1.8066(15)(16)			1.8040	1.8030	1.8032
D_1 $3s_{1/2}$-$3p_{1/2}$						
Hf^{61+}	8.1093(5)(15)	8.107(2)	8.1082(12)	8.1073	8.0944	8.1053
Ta^{62+}	7.9383(4)(15)	7.937(2)	7.9378(12)	7.9348	7.9241	7.9332
W^{63+}	7.7707(4)(15)	7.769(2)	7.7700(12)	7.7681	7.7587	7.7661
Au^{68+}	6.9991(5)(16)	6.999(2)	6.9991(12)	6.9974	7.0025	6.9973

=20 to Z=90; unfortunately, none of the elements of the present work were studied in Ref. [35]. Although both sets of calculated transition energies [34,35] agree quite well for medium Z, they diverge toward higher Z with Blundell's results showing better agreement with the most accurate results from the Livermore group for the D_2 line at Z=82 [14] and Z=92 [16]. Even better agreement is obtained at Z=92 by Chen *et al.* [37]. Near Z=80, the predicted QED contributions are approximately 3% (D_1) and 1% (D_2) of the transition energies and 0.1% of the splitting.

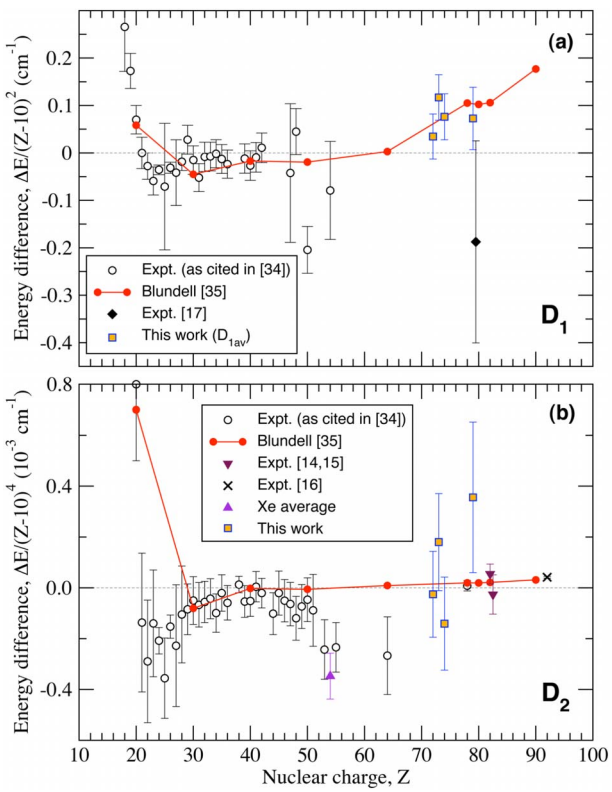

FIG. 2. (Color online) Comparison between experiments and prediction, $(E_{Kim}-E)/Z_c^{\alpha}$ for (a) D_1 line $3s_{1/2}$-$3p_{1/2}$, α=2, and (b) D_2 line $3s_{1/2}$-$3p_{3/2}$, α=4. Note: Refs. [15,17] shifted by +0.5 units of charge for a better visibility.

Our measured and calculated wavelengths of the D_1 and D_2 lines are listed in Table I and shown in Fig. 2 in comparison with the calculations of Kim *et al.* [34], Blundell [35], and all other available high-Z experiments [8–17,34]. Since the three Xe measurements [8–10] all agree very well with each other, we plot only their weighted average.

Lines from the lower ionization stages (Si-, Al-, and Mg-like) can also be seen near the D_2 line. In the Au spectrum, however, only the Mg-like line can be reliably identified since the higher beam energy (E=24 keV) effectively re-

TABLE II. Measured wavelengths (in nm) of spectral lines from Si-, Al-, and Mg-like ions and corresponding theoretical predictions.

Ion	This experiment	FAC	MCDF [38,39]
Si-like $3p^2(1/2,1/2)_0$-$3p3d(1/2,3/2)_1$			
Hf^{58+}	2.2184(9)(15)	2.2157	2.26058
Ta^{59+}	2.1192(18)(15)	2.1175	2.15935
W^{60+}	2.0257(10)(15)	2.0236	2.06262
Al-like $3p_{1/2}$-$3d_{3/2}$			
Hf^{59+}	2.2759(7)(15)	2.2743	2.27413
Ta^{60+}	2.1741(30)(15)	2.1716	2.17163
W^{61+}	2.0723(9)(15)	2.0736	2.07373
Mg-like $3s^2(1/2,1/2)_0$-$3s3p(1/2,3/2)_1$			
Hf^{60+}	2.5128(7)(15)	2.5096	
Ta^{61+}	2.3907(15)(15)	2.3868	
W^{62+}	2.2728(11)(15)	2.2702	
Au^{67+}	1.7751(15)(16)	1.7709	

duced the populations of Si- and Al-like ions. This analysis is confirmed by the modified intensity ratios for the group of lines near 7 nm. The measured wavelengths and identifications (in *jj*-coupling) of these $\Delta n=0$ transitions as well as the theoretical results obtained with the MCDF [38,39] and FAC codes are presented in Table II. Importantly, these lines span a narrow wavelength range, which makes them especially suitable for diagnostic purposes.

Prior to our work, most of the data in the range $Z=50-80$ were in disagreement with prediction, and none of the data in this range was accurate enough to distinguish between the two leading predictions, Kim *et al.* [34] and Blundell [35]. Furthermore, all of the significantly discrepant data in this range were *lower* in wavelength than theory, in contradiction to the x-ray results at much higher values of Z, which were *higher* in wavelength than theory. The results presented here for $Z=72$, 73, 74, and 79 favor the predictions of Blundell [35] over those of Kim *et al.* [34]. This significantly narrows the range of Z over which there exist discrepancies between theory and experiment and suggests that additional measurements in the range $Z=50-65$ would be valuable to determine whether the previous experiments there were affected by unaccounted for effects such as line blends. High-accuracy computations for more values of $Z>65$ would also be useful.

Supported in part by the Office of Fusion Energy Sciences of the (U.S.) Department of Energy. I.N.D. was supported by the Research Associate Program of the National Research Council. We thank B. Blagojević for helpful discussions in connection with the spectrometer.

[1] N. Ozaki, J. Appl. Phys. **42**, 3171 (1971).
[2] W. Ketterle, Rev. Mod. Phys. **74**, 1131 (2002).
[3] Yu. Ralchenko, A. E. Kramida, J. Reader, and NIST ASD Team (2008). NIST Atomic Spectra Database (version 3.1.5) (online). Available: http://physics.nist.gov/asd3 [2008, December 8]. National Institute of Standards and Technology, Gaithersburg, MD.
[4] U. Feldman, J. F. Seely, E. Landi, and Yu. Ralchenko, Nucl. Fusion **48**, 045004 (2008).
[5] C. Biedermann, R. Radtke, R. Seidel, and T. Pütterich, Phys. Scr. **T134**, 014026 (2009).
[6] J. M. Laming and U. Feldman, Astrophys. J. **527**, 461 (1999).
[7] R. D. Cowan, *The Theory of Atomic Structure and Spectra* (University of California Press, Berkeley, 1981).
[8] E. Trabert, P. Beiersdorfer, J. K. Lepson, and H. Chen, Phys. Rev. A **68**, 042501 (2003).
[9] K. Fahy, E. Sokell, G. O'Sullivan, A. Aguilar, J. M. Pomeroy, J. N. Tan, and J. D. Gillaspy, Phys. Rev. A **75**, 032520 (2007).
[10] J. F. Seely, U. Feldman, A. W. Wouters, J. L. Schwob, and S. Suckewer (unpublished).
[11] J. F. Seely, U. Feldman, C. M. Brown, M. C. Richardson, D. D. Dietrich, and W. E. Behring, J. Opt. Soc. Am. B **5**, 785 (1988).
[12] J. F. Seely, C. M. Brown, U. Feldman, J. O. Ekberg, C. J. Keane, B. J. MacGowan, D. R. Kania, and W. E. Behring, At. Data Nucl. Data Tables **47**, 1 (1991).
[13] T. E. Cowan, C. L. Bennett, D. D. Dietrich, J. V. Bixler, C. J. Hailey, J. R. Henderson, D. A. Knapp, M. A. Levine, R. E. Marrs, and M. B. Schneider, Phys. Rev. Lett. **66**, 1150 (1991).
[14] A. Simionovici, D. D. Dietrich, R. Keville, T. Cowan, P. Beiersdorfer, M. H. Chen, and S. A. Blundell, Phys. Rev. A **48**, 3056 (1993).
[15] P. Beiersdorfer and B. J. Wargelin, Rev. Sci. Instrum. **65**, 13 (1994).
[16] P. Beiersdorfer, E. Trabert, H. Chen, M.-H. Chen, M. J. May, and A. L. Osterheld, Phys. Rev. A **67**, 052103 (2003).
[17] E. Träbert, P. Beiersdorfer, E. H. Pinnington, S. B. Utter, M. J. Vilkas, and Y. Ishikawa, J. Phys.: Conf. Ser. **58**, 93 (2007).
[18] Yu. Ralchenko, I. N. Draganic, J. N. Tan, J. D. Gillaspy, J. M. Pomeroy, J. Reader, U. Feldman, and G. E. Holland, J. Phys. B **41**, 021003 (2008).
[19] G. E. Holland, C. N. Boyer, J. F. Seely, J. N. Tan, J. M. Pomeroy, and J. D. Gillaspy, Rev. Sci. Instrum. **76**, 073304 (2005).
[20] J. D. Gillaspy, Phys. Scr. **T65**, 168 (1996).
[21] M. A. Levine *et al.*, Nucl. Instrum. Methods Phys. Res. B **43**, 431 (1989).
[22] M. Matranga *et al.*, Nucl. Instrum. Methods Phys. Res. B **205**, 244 (2003).
[23] J. V. Porto, I. Kink, and J. D. Gillaspy, Rev. Sci. Instrum. **71**, 3050 (2000).
[24] B. Blagojevic *et al.*, Rev. Sci. Instrum. **76**, 083102 (2005).
[25] E. Silver *et al.*, Astrophys. J. **541**, 495 (2000).
[26] Yu. Ralchenko, J. Reader, J. M. Pomeroy, J. N. Tan, and J. D. Gillaspy, J. Phys. B **40**, 3861 (2007).
[27] Yu. Ralchenko, J. N. Tan, J. D. Gillaspy, J. M. Pomeroy, and E. Silver, Phys. Rev. A **74**, 042514 (2006).
[28] Yu. Ralchenko and Y. Maron, J. Quant. Spectrosc. Radiat. Transf. **71**, 609 (2001).
[29] M. F. Gu, Can. J. Phys. **86**, 675 (2008).
[30] W. Schwanda, K. Eidmann, and M. C. Richardson, J. X-Ray Sci. Technol. **4**, 8 (1993).
[31] B. L. Henke, E. M. Gullikson, and J. C. Davis, At. Data Nucl. Data Tables **54**, 181 (1993).
[32] L. Poletto, A. Boscolo, and G. Tondello, Appl. Opt. **38**, 29 (1999).
[33] J. Reader, V. Kaufman, J. Sugar, J. O. Eckberg, U. Feldman, C. M. Brown, J. F. Seely, and W. L. Rowan, J. Opt. Soc. Am. B **4**, 1821 (1987).
[34] Y.-K. Kim, D. H. Baik, P. Indelicato, and J. P. Desclaux, Phys. Rev. A **44**, 148 (1991).
[35] S. A. Blundell, Phys. Rev. A **47**, 1790 (1993).
[36] W. R. Johnson, S. A. Blundell, and J. Sapirstein, Phys. Rev. A **38**, 2699 (1988).
[37] M. H. Chen, K. T. Cheng, P. Beiersdorfer, and J. Sapirstein, Phys. Rev. A **68**, 022507 (2003).
[38] K.-N. Huang, At. Data Nucl. Data Tables **32**, 503 (1985).
[39] K.-N. Huang, At. Data Nucl. Data Tables **34**, 1 (1986).